Characterization of Linear Array Based on PZT Thick Film

Tomasz Zawada, Louise M. Bierregaard, Erling Ringgaard, Ruichao Xu, Michele Guizzetti

Meggitt A/S, Kvistgaard, Denmark
e-mail: tomasz.zawada@meggitt.com

Franck Levassort, Dominique Certon
University of Tours,
GREMAN UMR 7347 CNRS, Tours, France
e-mail: franck.levassort@univ-tours.fr

Abstract—**Multi-element transducers enabling novel cost-effective fabrication of imaging arrays for medical applications have been presented earlier. Due to favorable low lateral coupling of the printed PZT, the elements can be defined by the top electrode pattern, leading to a kerf-less design with low cross-talk between the elements. The linear arrays have proved to be compatible with a commercial ultrasonic scanner and to support linear array beamforming as well as phased array beamforming. The main objective of the presented work is to investigate the performance of the devices at the transducer level by extensive measurements of the prototype structures. The arrays have been characterized at the transducer level by several different measurement techniques. Firstly, electrical impedance measurements on several elements in air and liquid have been conducted. The arrays have also been characterized by a pulse-echo system. The measured sensitivity is around -60 dB, the fractional bandwidth is close to 60%, while the center frequency is about 12 MHz over the whole array. Finally, laser interferometry measurements have been conducted. The in-depth characterization of the array structure have given insight into the performance parameters for the array based on PZT thick film and the obtained information will be used to optimize the key parameters for the next generation of arrays based on piezoelectric thick film.**

Keywords—*PZT thick film, ultrasonic transducer, screen printing, array transducer, linear array, printed transducer*

I. INTRODUCTION

A tremendous increase of computational power and miniaturization of portable devices is currently driving the development in ultrasonic diagnostic instrumentation [1]. Need for new cost-effective manufacturing technologies and process is another major factor contributing to the current development trends. A significant effort goes into the development of Capacitive Micro-machined Ultrasonic Transducers [2], but this solution is mainly suitable for high volume products due to the need for very high upfront investments. Another trend, especially in higher frequency applications (above 20 MHz) is to down-scale the 2-2 composite technology combined with a heterogeneous integration approach, which in essence leads to increased production costs.

The detailed description of cost-effective solution based on screen printed multi-element arrays has been published earlier and the main objective of the presented work is to investigate deeper the electro-acoustic properties of PZT thick-film based acoustic arrays in order to aid the future design and optimization of similar structures.

The paper starts with an introduction to PZT thick film technology. Then the test structures of multi-element transducers are presented. This is followed by electric and electro-acoustic measurements using several techniques including laser interferometry as well as hydrophone characterization. Test results are then summarized together with an outlook for the future development.

II. PZT THICK FILM TEST STRUCTURES

The test structures have been fabricated using PZT thick film technology [3]. The transducer consists of an acoustically matched ceramic substrate, on which a bottom electrode, an active PZT layer and a top electrode are printed in consecutive steps. The thickness of the PZT layer has been chosen to be equal to 80 μm which corresponds to a center frequency of the transducer of around 11 MHz. The PZT thick films were then sintered at temperatures above 800 °C.

The transducers have been fabricated using a screen printing technique, where the gold bottom electrode has been deposited first, followed by deposition of the TF2100 PZT thick film. The top electrodes defining the elements of the array have been printed as well using silver fine line pattering. The pattern of the top electrode defines the 32-element array. A schematic cross-section of the fabricated device is given in Fig. 1. The effective length of the elements is 4.5 mm.
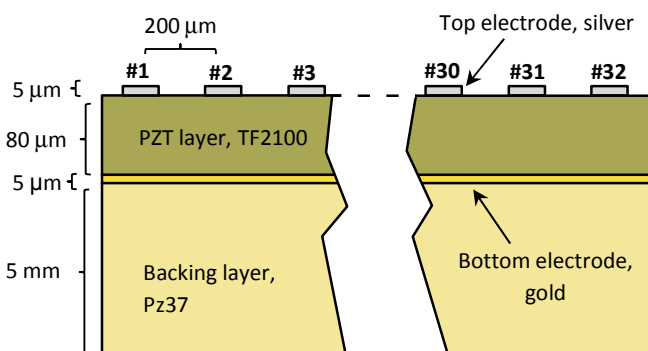

Fig. 1. Schematic cross-section of the fabricated multi-element transducer (not to scale)

The structures have been poled at elevated temperature using an electric field of 10 kV/mm.

Typically, the packaging and interconnect of multi-element transducers is one of the major technical challenges when it comes to design and manufacturing of array devices. The presented solution is based on the flip-chip technique where the functional device (chip) is connected to the PCB using solder bumps deposited on the top of the device. Hence the device is finally attached "upside down" with the active side facing the PCB. In the presented solution the top electrode pattern has been designed to match the pattern of conductive pads on a PCB carrier with an opening enabling acoustic coupling to the medium (Fig. 2). As a final step, a polymeric quarter-wave matching layer has been added.
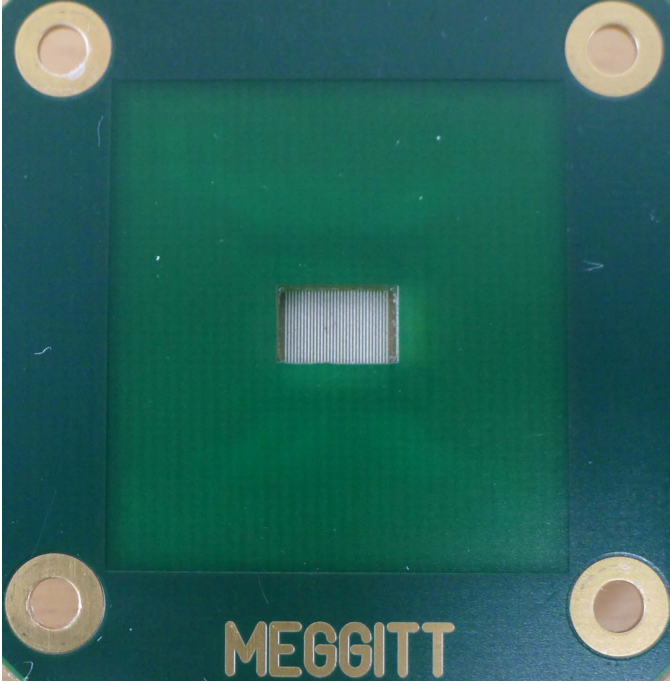

Fig. 2.   Top view of a PCB-packaged 32-element transducer

III.   CHARACTERISATION OF THE TEST DEVICES

A.   Electrical and electro-acoustic properties

Electrical impedance measurements have been performed using an HP4395A spectrum analyzer (Agilent, Palo Alto, CA) and an impedance test kit. All the elements were measured to evaluate the reproducibility and uniformity of the corresponding properties. Fig. 3 shows the superimposition of measured impedance in air of three representative elements and one element in water. All three measured elements deliver the same behavior and consequently they exhibit the same electromechanical properties.

Since the transducer consists of multiple layers, it is not trivial to determine the functional properties of the thick film itself, but in previous work on a similar film, the following parameters were determined using a multilayer KLM model [4]: acoustic impedance of 14.2 MRay, clamped relative permittivity $\varepsilon_{33}^{S}/\varepsilon_0$ of 316 and effective thickness coupling factor k_t of 0.44 [5].
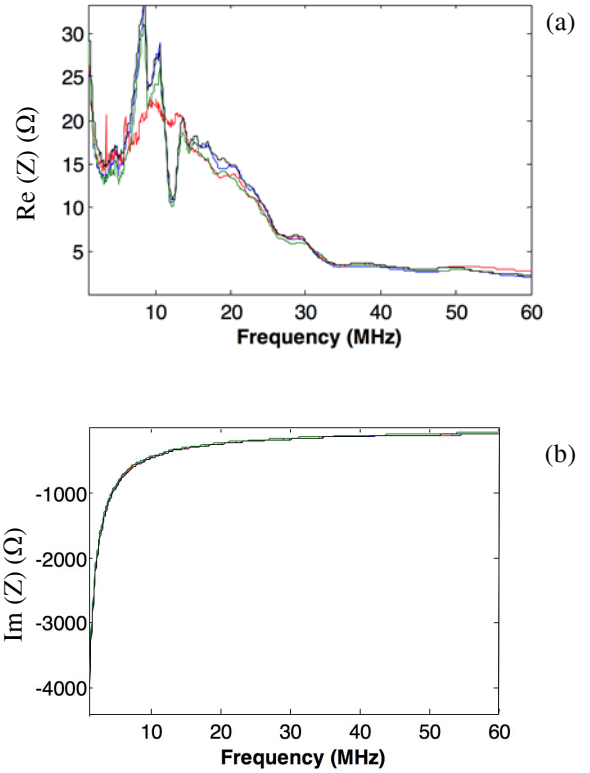

Fig. 3.   Complex electrical impedance (a: real part, b: imaginary part) versus frequency for three elements in air (blue: element number 16; green: element number 11; black: element number 32) and one element in water (red: element number 16)

Several elements of the linear array have been characterized using pulse-echo system with metallic target in water. An OLYMPUS (model 5077PR, Rungis, France) square wave pulser/receiver was used for the electrical excitation and reception. A 50 Ω cable around 50 cm in length was used. Fig. 4 represents the pulse-echo response of the element number 16.
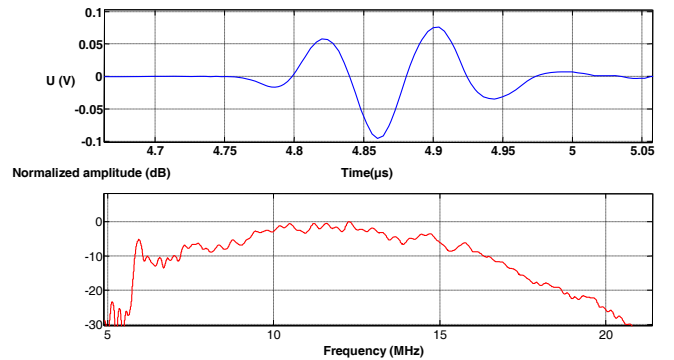

Fig. 4.   Pulse-echo response in time and frequency domain (element 16)

The insertion loss $IL=20\log(U_r/U_e)$, where U_r and U_e are the reception and excitation peak voltages, has been evaluated from the received voltage in pulse-echo mode and found to be equal to -60 dB for a center frequency at 12 MHz. The fractional bandwidths have been found at -6 dB and -20 dB at 41% and 106%, respectively.

B. Displacement measurements

The mechanical displacement of the array front face produced by excitation of one element was measured using laser interferometry (apparatus UHF-120 from Polytec SA, Waldbronn, Germany). The displacement has been scanned along a line placed at the center of the elevation, with a step of 20 µm, over a range of 2 mm from either side of the excited element. Electrical excitation conditions were the same as the ones used for pulse-echo experiments. Fig. 5 shows the displacement scan obtained. The small blue spot placed at zero laser spot position corresponds to the displacement measured on the excited element, and outside this is the displacement produced on neighboring elements by mechanical crosstalk. Fig. 5 shows two interesting features; firstly the amplitude of the displacement measured on the excited element reaches 20 nm which is quite significant, given the fact that the element has been fabricated using printing technology. Secondly, the width (160 µm) of the blue spot corresponding to the element excited agrees very well with the pitch of the device (200 µm). This aspect shows that the level of electrostatic crosstalk inside the array structure is low. Moreover, the very short pulse duration measured (110 ns) confirms the high level of damping obtained with the porous backing.

Note that the mechanical displacement amplitude produced by crosstalk could seem important with regard to the displacement measured on the element, but here the amplitude is overestimated due to acousto-optic interactions (Fig. 5) and is not significant [6]. Moreover, because the phase velocity of these waves is lower than ultrasonic velocity in water, the mechanical crosstalk is not radiated and does not contribute to the far field pressure.
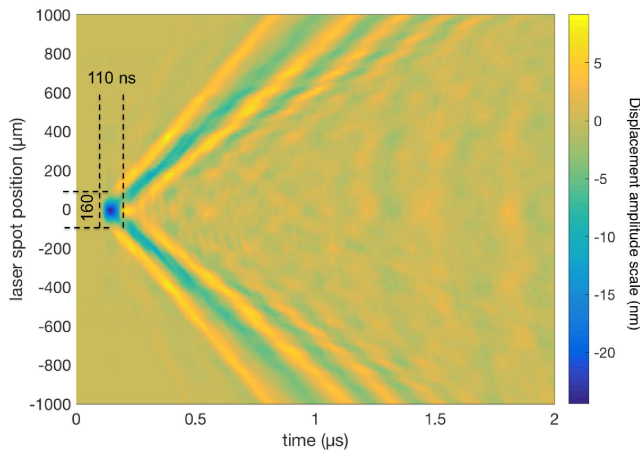

Fig. 5. Scan of the displacement collected at the surface of the array when one element is electrically excited

C. Hydrophone measurements

The pressure field radiated by one element has been characterized by using a hydrophone setup (Calibrated Needle hydrophone, HN series from Onda Corporation, Sunnyvale, USA). Excitation conditions were kept similar to those described in the previous section. In the first step, the far field pressure emitted (at 40 mm from the array) was measured and

the results are presented in Fig. 6. The central frequency has been found to be equal to 9.5 MHz with a corresponding fractional bandwidth of 55 % at -3dB. One can note the significant peak-to-peak amplitude of the pressure, close to 200 kPa for one element. In comparison with the pulse-echo measurements, the central frequency seems lower in emission. This is due to the existence of a strong cut-off frequency at 16 MHz that is not observed on the pulse-echo signal. At this stage of this study, no clear hypothesis can be provided to explain such cut-off frequency except, probably, the operating conditions. For pulse-echo measurements a 50 Ω cable of 50 cm length was used, while for hydrophone measurements a longer cable (1.5 m) was required.
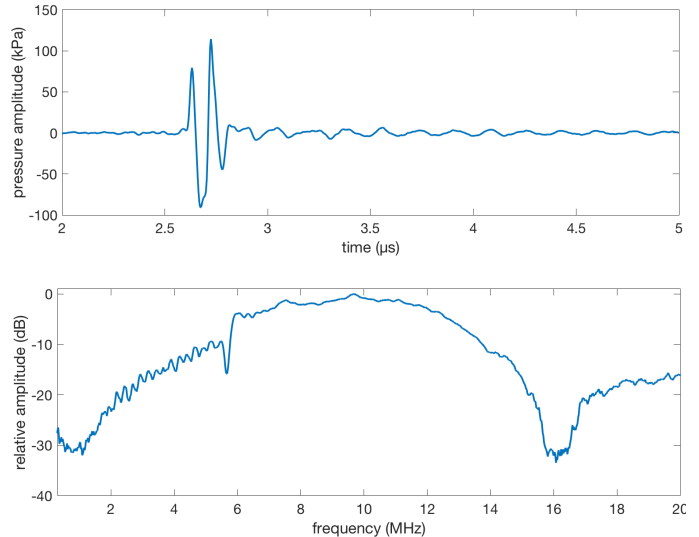

Fig. 6. Pressure measured at 40 mm from the array (a) time response and (b) spectrum. The central frequency at -3dB is 9.5 MHz and the corresponding fractional bandwidth is 55 %

A scan of the pressure at 4 mm from a selected element along a line parallel to the array has been performed. The hydrophone was mechanically moved with a step of 250 µm. Results are presented in Fig. 7. One can note the pressure amplitude at the probe output: more than 300 kPa peak-to-peak (at 10 MHz) for one emitter only. This value is quite significant and comparable with performances of commercially available probes.

Fig. 8 presents a pressure scan illustrating variations of the peak-to-peak amplitude against the hydrophone position. The quantity obtained theoretically is superimposed on the experimental results. The theoretical curve has been computed by simulating the pressure field radiated by a piston-like square shape acoustic source, with 160 µm width and 4 mm in elevation. Theory and experiments agree very well up to 4 mm. This confirms the very low level of mechanical crosstalk inside the structure, and that its contribution in the far field is null. Beyond 4 mm discrepancies with experiments are due to the hydrophone size, i.e. 200 µm which has not been considered in the described simulation.
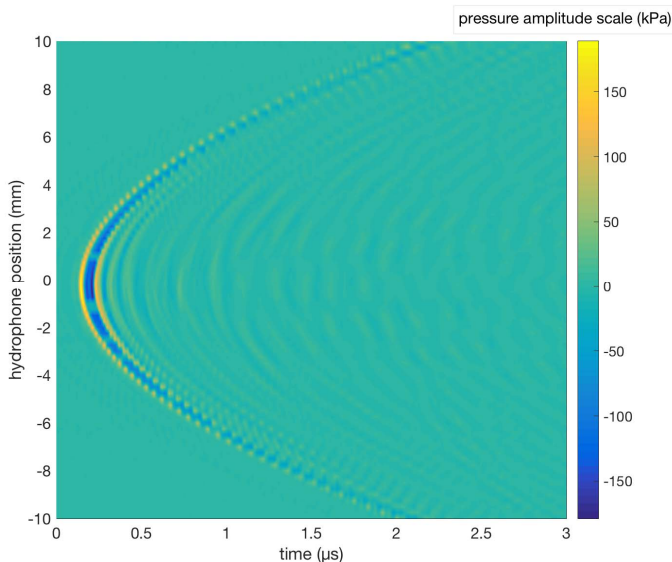
Fig. 7. Pressure measured along line parallel to the array at a distance of 4 mm
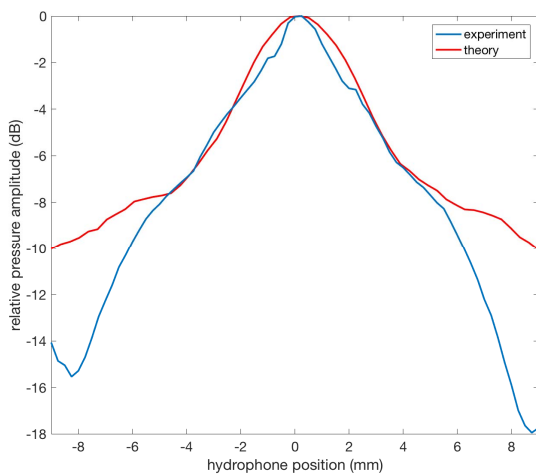

Fig. 8. Variations of the peak-to-peak amplitude against hydrophone position along a line parallel to the array, at distance of 4 mm

IV. CONCLUSIONS AND OUTLOOK

Ultrasonic transducer arrays with 32 elements have been successfully manufactured using a kerf-less PZT thick-film technology, and functional characterization of the test devices has been carried out using a number of experimental and analytical methods.

Impedance measurements show good uniformity throughout the arrays, and pulse-echo measurements yield a quite respectable insertion loss of -60 dB. The corresponding center frequency is equal to 12 MHz, and fractional bandwidths are 41% and 106% at -6 dB and -20 dB, respectively.

Displacement at the surface of the array measured by laser interferometry is equal to approximately 20 nm. Furthermore, interferometry measurements have confirmed that the mechanical cross-talk between the elements is low and the short pulse duration of 110 ns is evidence that the porous backing provides proper damping.

Measurements with a needle hydrophone show a peak-to-peak acoustic pressure as high as 300 kPa at 10 MHz. Moreover, the good agreement between the peak-to-peak amplitude variation with hydrophone position and a simulated curve confirms once more that the level of mechanical crosstalk inside the structure is very low, and that its contribution in the far field can be neglected.

In conclusion the characterization shows that the performance of the thick-film arrays is comparable to state-of-the-art commercial transducers. It is worth noting that this is obtained with a technology characterized by low upfront investments, yet allowing up-scaling and manufacturing at very competitive price.

An important task for future work will be to further increase the number of elements. Even though the basic imaging functionality using commercial scanner has already been demonstrated [3], the significantly enhanced image quality resulting from a higher number of elements will make the presented technology even more competitive to today's state-of-the-art solutions.

REFERENCES

[1] T.L. Szabo, Diagnostic Ultrasound Imaging: Inside Out, 2nd ed. Oxford: Academic Press, 2014, pp. 366-369.

[2] B.T. Khuri-Yakub and Ö. Oralkan, "Capacitive micromachined ultrasonic transducers for medical imaging and therapy", J. Micromech. Microeng., vol. 21.5, pp. 054004–054014, 2011.

[3] L. M. Bierregaard, T. Zawada, E.Ringgaard, R. Xu, M. Guizzetti, J. P. Bagge, L. N. Moesner, "Cost-effective screen printed linear arrays for medical imaging fabricated using PZT thick films", in Proc. 2015 IEEE Ultrasonics Symposium, pp. 109-112, 2015.

[4] D. Leedom, R. Krimholtz, and G. Matthaei, "New equivalent circuits for elementary piezoelectric transducers," Electronics Letters, vol. 6, no. 13, pp. 398–399, 1970.

[5] A. Guiroy, A. Novell, E. Ringgaard, R. Lou-Moeller, J.M. Grégoire, A.-P. Abellard, T. Zawada, A. Bouakaz, F. Levassort, "Dual-frequency transducer for nonlinear contrast agent imaging", IEEE Trans. Ultrason., Ferroelect., Freq. Contr., 60 [12] 2634-2644, 2013.

[6] D. Certon, G. Férin, O. Boumatar, JP. Remenieras, F. Patat, "Influence of acousto-optic interactions on the determination of the diffracted field by an array obtained from displacement measurements". Ultrasonics, 42: pp. 465-471, 2004.